ELSEVIER

Journal of Molecular Catalysis A: Chemical 118 (1997) 33–45

JOURNAL OF MOLECULAR CATALYSIS A: CHEMICAL

Multiple bonds between transition metals and main-group elements: Part 161 [1] Oxygen-donor adducts of organorhenium(VII) oxides: syntheses, structures and catalytic properties

Wolfgang A. Herrmann *, João D.G. Correia, Monika U. Rauch, Georg R.J. Artus, Fritz E. Kühn

Anorganisch-chemisches Institut der Technischen Universität München, Lichtenbergstraße 4, 85747 Garching bei München, Germany

Received 2 April 1996; accepted 9 August 1996

Abstract

N-Oxide adducts of methyltrioxorhenium(VII) (**1**) are characterized and their catalytic properties in the epoxidation of olefins with hydrogen peroxide are examined. The crystal structure of one of these derivatives is described. Whereas aliphatic *N*-oxides form temperature-sensitive adducts with **1** and are inactive in the catalytic epoxidation of olefins, aromatic *N*-oxides adducts of **1** are both stable and catalytically active. The latter complexes show lower activity than **1**, but in some cases the selectivity is even higher than that of the *N*-base adducts of **1**. The catalytic active species are of similar type in all examined cases. The structure of the oxo-functionalized complex $[O_3Re(CH_2)_2CH(CH_3)OCH_3]$ as well as its catalytic properties in the olefin epoxidation with hydrogen peroxide are reported. The deactivation process of this catalyst is also examined.

Keywords: Catalysis; Olefins; Oxidation; Peroxo complexes; Rhenium; X-ray structures

1. Introduction

Organorhenium(VII) oxides have proven to be very efficient catalysts in many different catalytic processes [1–27]. Especially the system methyltrioxorhenium (**1**)/H_2O_2 has been extensively studied during the last years [1–27]. Catalytic active species, $CH_3ReO(O_2)_2 \cdot L$ (L = H_2O (**2a**), $OP(N(CH_3))_3$) (**2b**), have been isolated and characterized [25,28]. Higher homologues of **1** are more temperature sensitive and form less stable and efficient catalysts in the presence of H_2O_2 [25,29,30]. A structurally similar, but much more water sensitive and therefore a less efficient catalyst is formed by the reaction of Re_2O_7 with H_2O_2 ($O[ReO(O_2)_2 \cdot H_2O]_2$) [31]. Despite the high activiy of **2a** in the olefin oxidation it has been shown that the addition of Lewis bases, e.g., quinuclidine, to this catalyst leads to an improved selectivity

* Corresponding author.

[1] Communication 160 of this Series: M.H.P. Rietveld, L. Nagelholt, D.M. Grove, N. Veldman, A.L. Spek, M.U. Rauch, W.A. Herrmann, G. van Koten, J. Organomet. Chem. (1996), in press.

PII S1381-1169(96)00377-9

(decrease of the Lewis acidity of the metal center), but reduced activity in the catalytic epoxidation of olefins [26]. Addition of nitrogen Lewis bases to other alkylrhenium(VII) oxides not only improves their stability but also their lifetime under catalytic conditions [26,29]. It has been shown recently that the quinuclidine adduct of cyclopropyltrioxorhenium(VII) is an even more efficient oxidation catalyst in the presence of H_2O_2 than the analogous complex of **1** [26].

Having in mind the aforementioned results, intramolecular *N*-donor adducts of organorhenium(VII) oxides, e.g., $O_3Re-(CH_2)_3N(C_5H_{10})$ [26,32], were synthesized. However, these type of complexes are inactive in oxidation catalysis [33]. ^{17}O NMR studies have indicated that *O*-donors form somewhat weaker complexes with organorhenium(VII) oxides than *N*-donors and may therefore present higher catalytic activities than their *N*-containing congeners [32,34].

In this work we present the syntheses, structures and catalytic properties of new inter- and intramolecular *O*-donor complexes of organorhenium(VII) oxides.

2. Results and discussion

2.1. Synthesis and spectroscopy of N-oxide adducts of methyltrioxorhenium(VII)

Reaction of **1** with different *N*-oxides in acetonitrile or diethyl ether at low temperatures leads to quantitative formation of the adducts as pale-yellow precipitates within minutes (Scheme 1). Trimethylamine *N*-oxide, quinuclidine *N*-oxide, 4-*tert*-butylpyridine *N*-oxide and (rac)-[1-(6-bromopyrydine-2-yl*N*-oxide)-2,2-dimethyl-propyl]methyl ether were used to obtain the complexes **3a–3d**.

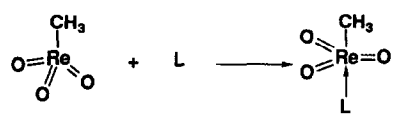

1 3a-3d

Scheme 1.

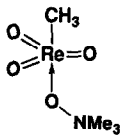

3a

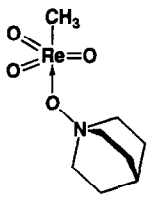

3b

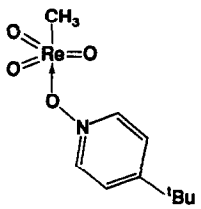

3c

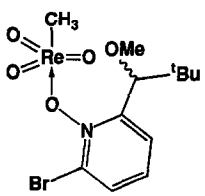

3d

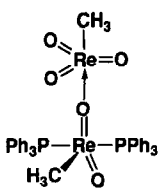

4

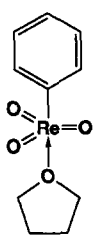

5

While **3a** and **3b** are temperature and moisture sensitive, **3c** is stable at ambient temperature and in air for some hours. Decomposition of compound **3a–3d** in laboratory atmosphere leads to the formation of perrhenates, easily detectable by the formation of white precipitates and their characteristic IR and ^{17}O NMR spectra [34,35].

Complexes **3a–3d** are among the first monomeric *O*-donor adducts of organorhenium(VII) oxides, in fact only two other examples have been structurally characterized previously, namely $CH_3ReO_3 \cdot [ORe(O)(PPh_3)_2-(CH_3)]$ (**4**) [36] and $C_6H_5ReO_3 \cdot THF$ (**5**) [37].

In the IR spectra of the complexes **3a–3d** the symmetric and asymmetric Re=O stretching frequencies are shifted to lower wavenumbers (ν_{sym} ca. 965 cm^{-1} (KBr), ν_{asym} ca. 915–930 cm^{-1} (KBr)) compared to **1** (ν_{sym}(Re=O) = 998 cm^{-1} (KBr), ν_{asym}(Re=O) = 959 cm^{-1} (KBr) [38]). The chemical shift is comparable to that of monodentate *N*-base adducts of **1** [27,34]. This result indicates a comparable donor capability of the *O*-donors and *N*-donors. The Re=O bond strength is weakened by the additional donor ligand in the complexes **3a** – **3d** [27].

^{17}O NMR spectroscopy shows a similar view: while **1** exhibits a signal at $\delta(^{17}O) = 822$ ppm ($\Delta\nu_{1/2} = 130$ Hz) [8] for the terminal oxygen atoms, complexes **3a** – **3d** show singlets around $\delta(^{17}O) \approx 840$ ppm ($\Delta\nu_{1/2} \approx 200$ Hz) for the terminal oxygens at room temperature ($CDCl_3$). This indicates a *higher* electron density on the terminal oxygen atoms and consequently a weakening of the Re=O bond in comparison with not coordinated **1**, as described elsewhere [34]. If one equivalent of free quinuclidine is added to a solution of **3b** in $CDCl_3$ at room temperature a second peak ($\delta(^{17}O) = 906$ ppm) can be observed, due to the formation of the quinuclidine adduct of **1** (**1a**). The original peak at 840 ppm broadens significantly, but both peaks are of approximately the same heigth and half widths (ca. 900 Hz). If the solution is warmed to 55°C the two peaks coalesce to one very broad signal, approximately in the middle of the two former peaks. These results clearly indicate an exchange of the *N*- and *O*-donor ligands, as depicted in Scheme 2, and confirm the assumption that the Re–N and Re–O bonds are of comparable strength. A similar process can be observed by treating a solution of **3c** ($\delta(^{17}O) = 841$ ppm, $\Delta\nu_{1/2} = 216$ Hz) with 4-*tert*-butylpyridine.

2.2. Solid state structure of (4-tert-butylpyridine N-oxide)methyltrioxorhenium(VII) (3c)

As an example for *N*-oxide complexes of methyltrioxorhenium, **3c** has been examined by means of a X-ray structure determination. The structure of **3c** is shown in Fig. 1. The compound exhibits a trigonal bipyramidal geometry. As it is known for most structurally characterized intermolecular *N*-base adducts the terminal oxygen atoms occupy equatorial positions. The average C–Re–O(equ) angle is 96.7° and of the same magnitude as in the aforementioned *N*-base adducts (average C–Re–O(equ) = 97° [27,35]). The Re–C distance is 209.6(9) pm and thus prolongated in comparison to **1** *d*(Re–C) = 206.3(2) pm [27], but again similar to *N*-base complexes of **1** (average *d*(Re–C) = 209 pm) [27,35]. The Re=O bond distance remains unchanged at 169 pm. The Re–O4 distance (231.1(4) pm) is much shorter than the average Re–N bond distance in *N*-base adducts of organorhenium(VII) oxides (242 pm, [27]) and also notably shorter than the Re–O bond dis-

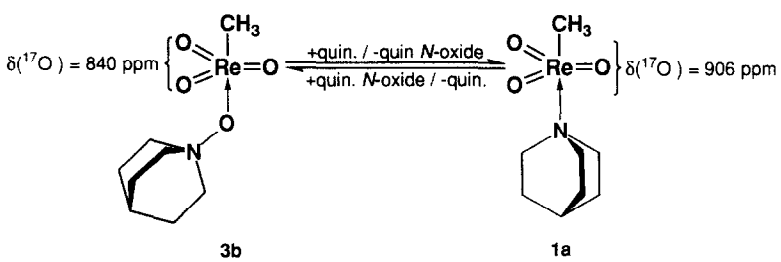

Scheme 2.

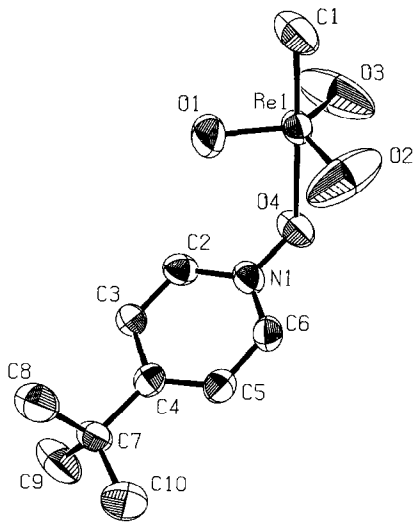

Fig. 1. PLATON representation [51] of (4-*tert*-butylpyridine *N*-oxide)methyl trioxorhenium **3c** in the solid state (single-crystal X-ray diffraction). Thermal ellipsoids are at 50% probability level. Hydrogen atoms are omitted for clarity. Selected bond lengths (pm) and angles (°): Re(1)–O(1) 168.8(6); Re(1)–O(2) 167.6(7); Re(1)–O(3) 169.6(7); Re(1)–O(4) 231.1(4); Re(1)–C(1) 209.6(9); O(4)–N(1) 134.4(7); O(1)–Re(1)–O(2) 116.8(6); O(1)–Re(1)–O(3) 119.6(5); O(2)–Re(1)–O(4) 83.3(3); O(2)–Re(1)–C(1) 98.8(4); O(4)–Re(1)–C(1) 178.0(4); Re(1)–O(4)–N(1) 115.1(3); O(4)–N(1)–C(2) 118.5(6); C(2)–N(1)–C(6) 120.8(6).

tance in both known organorhenium(VII)–oxygen donor complexes (**4**: d(Re–O) = 237.7(7) pm [36], **5**: d(Re–O) = 242.0(2) pm [37]). This is probably due to the smaller steric demand and the better donor qualities of an *N*-oxide compared to donor solvents, e.g., THF. Nevertheless, the Re–O(ligand) bond distance in **3c** is much longer than the sum of the covalence radii of the atoms and therefore indicates a still relatively weak interaction. This is in good accordance with the results obtained from the ligand exchange experiments described in Section 2.1.

2.3. Catalytic properties of the N-oxide adducts of methyltrioxorhenium(VII)

The catalytic properties of the *N*-oxide adducts of methyltrioxorhenium were tested in the oxidation of cyclohexene with H_2O_2 in *tert*-butanol at 25°C (Scheme 3). The catalytic properties of these compounds were compared

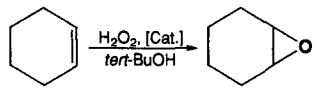

Scheme 3.

with those of the *N*-donor adducts of methyltrioxorhenium.

Unlike $CH_3ReO_3 \cdot$ (4-*t*bupy) (**1b**), $CH_3ReO_3 \cdot$ (4-*t*bupy *N*-oxide) (**3c**) appears as a selective oxidation catalyst of olefins (Fig. 2). No oxirane ring-opening is observed, even after 24 h. The selectivity of **3c** is similar to that reached with $CH_3ReO_3 \cdot$ (quin.) (**1a**). However, when the latter is used as catalyst, a higher activity (100% yield, ≈ 1.5 h) is observed.

The aliphatic *N*-oxide adducts of CH_3ReO_3, $CH_3ReO_3 \cdot$ (quin.*N*-oxide) (**3b**) and $CH_3ReO_3 \cdot$ (trimethylamine*N*-oxide) (**3a**), do not show any catalytic activity in the oxidation of olefins. This is not surprising since such adducts decompose easily in the presence of water, yielding perrhenate ($\delta(^{17}O) = 560$ ppm, $CDCl_3$, 25°C) at room temperature. Thus, the catalysts are destroyed by hydrogen peroxide. However, catalytic activity is observed when excess quinuclidine *N*-oxide (5 equiv.) is added to a solution where the active species was already formed. This result indicates that $CH_3(O)Re(O_2)_2 \cdot H_2O$ is stable in the presence of aliphatic *N*-oxides. A stable complex of the type $CH_3(O)Re(O_2)_2 \cdot$ (quin. *N*-oxide) is probably formed.

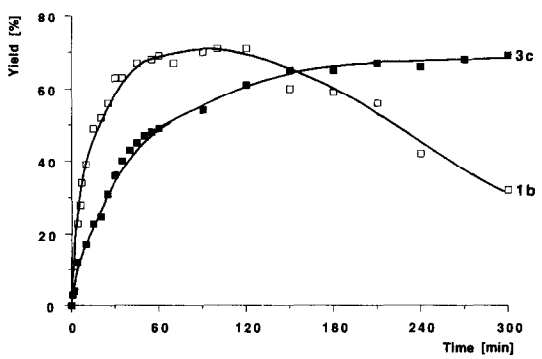

Fig. 2. Catalytic activity of $CH_3ReO_3 \cdot$(4-*t*bupy *N* oxide) (***3c***), and $CH_3ReO_3 \cdot$(4-*t*bupy) (***1b***) in the oxidation of cyclohexene to epoxycyclohexane with H_2O_2. Cyclohexene: H_2O_2:[Cat.] = 1:1.5:0.01; T = 25°C.

Comparing the systems in which excess bidentate Lewis-bases are used [CH_3ReO_3:2,2′-bipy *N,N′*-dioxide = 1:6 (**a**), and CH_3ReO_3:2,2′-bipy = 1:6 (**b**)], shows that the total amount of formed epoxycyclohexane is almost the same in both cases (Fig. 3). However, when *N,N′*-dioxide is employed no oxirane ring-opening is observed. In the case of the CH_3ReO_3/2,2′-bipy system a small amount of 1,2-cyclohexanediol was detected after ca. 2 h. 2,2′-bipy *N,N′*-dioxide leads to slightly better selectivities than 2,2′-bipy.

The system **3d**/H_2O_2 presents a high activity in the oxidation of olefins to epoxides with hydrogen peroxide (100% conversion after 1 h), but no selectivity is achieved. Only products resulting from the oxirane ring-opening are observed after the reaction. The very bulky rac-[1-(6-bromopyridine-2-yl*N*-oxide)-2,2-dimethylpropyl]methyl ether in complex **3d** is obviously weakly coordinated to the rhenium center due to sterical reasons, which means that the Lewis-acidity of the metal is still high enough to allow the oxirane-ring opening.

2.3.1. Active species of the system CH_3ReO_3/ H_2O_2 / 4-tert-butylpyridineN-oxide. Synthesis and spectroscopy

(4-*tert*-Butylpyridine *N*-oxide)methyl (oxo)bis(η^2-peroxo)rhenium(VII) (**2c**) was prepared by addition of a solution of 4-*tert*-butylpyridine*N*-oxide in CH_2Cl_2 (1 equiv.) to a solution of **2a** in diethyl ether at 0°C. A red-orange solid precipitated immediately (Scheme 4). After filtration and washing of the remaining solid with diethyl ether and pentane **2c** was dried in vacuo.

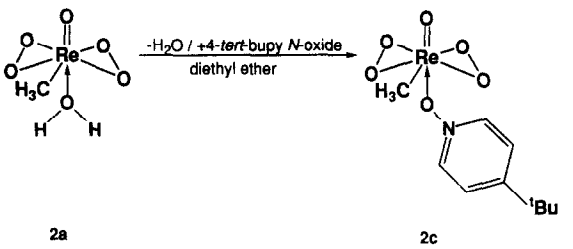

Scheme 4.

The bis(peroxo) complex **2c** is soluble in methylene chloride and water but, unlike **2a**, it is insoluble in diethyl ether. It is less hygroscopic than **2a**, and melts at 95–96°C under decomposition.

The IR spectrum (CH_2Cl_2) shows the absorption bands of the terminal oxo ligand (ν(Re=O) = 992 cm^{-1}), the η^2-peroxo groups ($\nu(O_2)$ = 871, 849, 823 cm^{-1}) and a band corresponding to the coordinated *N*-oxide molecule (ν(Re–O–N) = 1492 cm^{-1}). Bands corresponding to ReOOH groups are not observed.

In the ^{17}O NMR spectra, the signal of the oxo ligands (Re=O) of in situ generated **2c** ($\delta(^{17}O)$ = 758 ppm, $CDCl_3$, −25°C) is nearly identical to that of **2a** ($\delta(^{17}O)$ = 760 ppm, $CDCl_3$, −25°C). However, in the ^1H NMR the protons of the methyl group in isolated **2c** are shifted to lower field ($\delta(^1H)$ = 2.89 ppm) compared to the same signal in **2a** ($\delta(^1H)$ = 2.60 ppm).

The bis(peroxo) complex **2c** reacts stoichiometrically with *cis*-cyclooctene in dry THF at room temperature, yielding epoxycyclooctane quantitatively in the same way as previously described for **2a**. This observation is a clear evidence for the presence of an oxidative active compound containing two η^2-peroxo groups in the catalytic cycle.

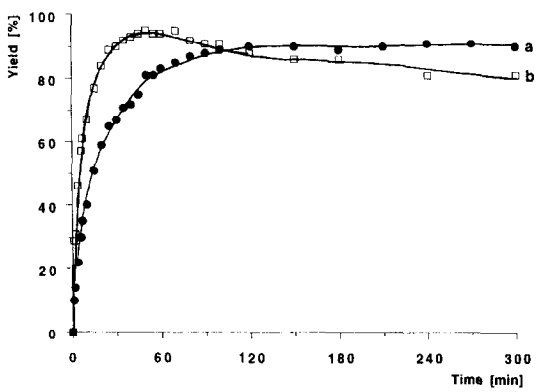

Fig. 3. Catalytic activity of CH_3ReO_3:2,2′-bipy *N,N′*-dioxide = 1:6 (*a*), and CH_3ReO_3:2,2′-bipy = 1:6 (*b*) in the oxidation of cyclohexene to epoxycyclohexane with H_2O_2. Cyclohexene: H_2O_2:[Cat.] = 1:1.5:0.01; *T* = 25°C.

2.4. Synthesis, spectroscopy and structure of [3-methoxy-n-butyl]trioxorhenium(VII) (6)

The reaction of dirheniumheptaoxide with bis(3-methoxy-*n*-butyl)zinc in THF at low temperatures yields the dimeric form of [3-methoxy-*n*-butyl]trioxorhenium(VII) (**6**) in 75% yield according to Scheme 5. Compound **6** is a pale-yellow solid which decomposes at 72°C. In spite of being less stable than the related monomeric amino-functionalized derivatives, $O_3Re(CH_2)_3NC_5H_{10}$ (**7a**) and $O_3Re(CH_2)_3N(C_2H_5)_2$ (**7b**) [26,32], compound **6** is much more stable than the not intramolecularly stabilized long chain alkylrhenium(VII) oxides derivatives (e.g., propyl- and pentyltrioxorhenium [29]).

The IR spectrum (KBr) shows the Re=O stretching frequencies at 972 and 940 cm^{-1}. Compared to the alkylrhenium(VII) oxides, these frequencies are shifted to lower wavenumbers, indicating weaker Re=O interactions [27]. The frequencies are comparable to those of intermolecular Lewis-base adducts of organorhenium(VII) oxides [4,9].

The ^{17}O NMR spectrum of compound **6** was reported previously [32]. The results of temperature-dependent measurements and studies in the presence of *N*-donors (e.g., quinuclidine) showed a comparatively weak intramolecular Re–O(ether) interaction and a fluxional coordination geometry in solution [32].

In mass spectroscopy (CI and EI-MS, respectively) a strong molecular peak for the monomer of **6** is obtained. This is in remarkable contrast to the long chain alkylrhenium(VII) oxides where only very small or no molecular peaks can be observed [35]. In the case of the intermolecular Lewis-base adducts of alkylrhenium(VII) oxides molecular peaks were never obtained under CI or EI-MS conditions [35]. This is again an indication for the stabilizing effect of an intramolecular donor ligand.

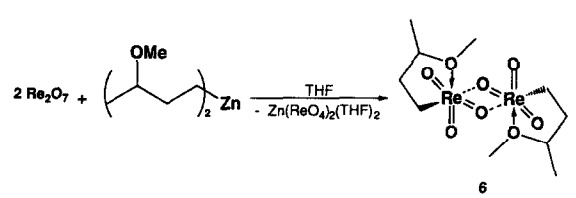

Scheme 5.

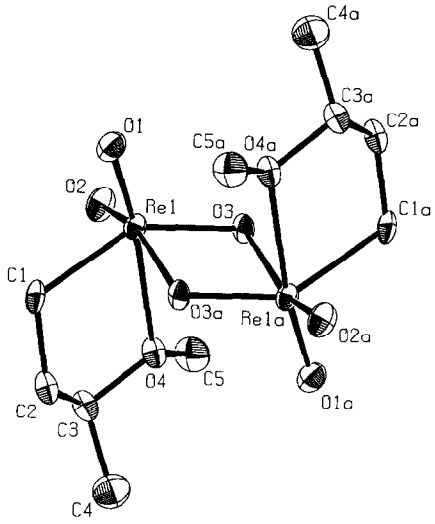

Fig. 4. PLATON representation [51] of (3-methoxy-*n*-butyl)trioxorhenium(VII) **6** in the solid state (single-crystal X-ray diffraction). Thermal ellipsoids are at 50% probability level. Hydrogen atoms are omitted for clarity. Atoms marked '*a*' are produced by an inversion center. Selected bond lengths (pm) and angles (°): Re(1)–O(1) 169.1(5); Re(1)–O(2) 170.7(4); Re(1)–O(3) 184.8(4); Re(1)–O(4) 235.7(5); Re(1)–C(1) 214.0(7); O(2)–Re(1)–O(1) 104.6(2); O(3)–Re(1)–O(1) 108.6(2); O(3)–Re(1)–O(2) 103.7(2); O(4)–Re(1)–O(1) 168.5(2); C(1)–Re(1)–O(3) 143.8(2); C(1)–Re(1)–O(3a) 77.0(2); O(4)–Re(1)–O(2) 81.6(2); O(4)–Re(1)–O(3) 78.6(2); C(1)–Re(1)–O(1) 95.5(2); C(1)–Re(1)–O(2) 95.4(3); C(1)–Re(1)–O(4) 74.1(2).

Single crystals of **6** were obtained by crystallization at −30°C in THF. The structure of **6** is shown in Fig. 4. In contrast to **7a** and **7b** and all other previously examined complexes of alkylrhenium(VII) oxides, **6** forms a dimer. The structure consists of two distorted, edge sharing octahedrons with a crystallographic inversion center on the common edge. The Re–O bond distances to the bridging oxo ligands are significantly longer than to the terminal oxo ligands (210.5(4) pm and 184.8(4) pm vs. 170.7(4) pm and 169.1(5) pm). The Re1–C1 bond distance is of similar length as in the compounds **7a** and **7b** and also clearly longer than in **1** or intramolec-

ular adducts of **1**. The Re1–O4 bond distance is relatively short (235.7(5) pm) and therefore comparable to the bond length in complex **3c** (see above). Contrary to the intermolecular *trans*-adducts of **1** the distances Re–O and Re–N are similar in the intramolecular *cis*-adducts **6**, **7a** (238.7(4) pm) and **7b** (238.3(3) pm). A possible reason for the dimerization of **6** might be the weaker donor capability of an ether function compared to amines, which would lead to an electronically less saturated rhenium center in the monomeric form of **6**. So far, only very few dimeric rhenium(VII) oxide complexes with a similar structure are known, e.g., the methanol adduct of methoxytrioxorhenium(VII) [39].

2.5. Properties of [3-methoxy-n-butyl]trioxorhenium(VII) (6)

2.5.1. Reaction of [3-methoxy-n-butyl]trioxorhenium(VII) (6) with H_2O_2

Addition of H_2O_2 (10% wgt in THF) to a colorless solution of **6** in THF leads to a bright yellow color within a few minutes. The reaction is significantly slower than the reaction of **1** with H_2O_2. The formation of a new complex can be monitored by ^{17}O NMR spectroscopy: the signal of **6** at $\delta(^{17}O) = 802$ ppm disappears and a new signal, ascribed to a peroxo species, appears at $\delta(^{17}O) = 732$ ppm. This chemical shift is comparable to that of **2a** [31–34].

Compound **6** exhibits two absorption bands in the UV/Vis spectrum at $\lambda_{max} = 250$ nm and 296 nm. The latter signal results from a LMCT transition of an intramolecular donor interaction [26]. The appearance of the UV/Vis spectrum of **6** is similar to that of **7a, b** [26,32].

The reaction observed in the ^{17}O NMR spectrum can also be detected in the UV/Vis spectrum: Addition of H_2O_2 to **6** leads to a new band at $\lambda_{max} = 356$ nm ($\epsilon = 600\ l\,mol^{-1}\,cm^{-1}$, THF). This band resembles the absorption band of **2a** ($\lambda_{max} = 364$ nm, $\epsilon = 700\ l\,mol^{-1}\,cm^{-1}$, THF) [25,26].

As in the case of the system $1/H_2O_2$, the system $6/H_2O_2$ decomposes without detectable intermediates (Fig. 5) to perrhenic acid. If excess H_2O_2 is used, the lifetime of the system is much higher. The decomposition process of $6/H_2O_2$ follows a pseudo first-order reaction. The rate constant ($k = 7.6 \times 10^{-5}\ 1\,s^{-1}$, 24°C) for that process is of the same order as that for the decomposition process of $1/H_2O_2$ ($k = 2.4 \times 10^{-5}\ 1\,s^{-1}$, 24°C), and the activation energy (E_a) is 67 kJ/mol).

2.5.2. Catalytic properties of [3-Methoxy-n-butyl]trioxorhenium(VII) (6)

The oxidation of *cis*-cyclooctene with hydrogen peroxide (10% wgt. in THF) catalyzed by **6** (1 mol%) at room temperature, yields epoxycyclooctane in 36% yield after ca. 60 min (Scheme 6).

Under comparable conditions, cyclohexene is converted in 20% to a mixture of epoxycyclohexane (50%) and 1,2-cyclohexanediol (50%). The system $6/H_2O_2$ is significantly more selective than $1/H_2O_2$ (only 1,2-cyclohehexanediol is obtained under comparable conditions) but less active at room temperature. As seen, the hydrolytic oxirane ring-opening is not completely avoided with the system $6/H_2O_2$. This constitutes a disadvantage in comparison to most of the *N*-base adducts of **1** and shows again the somewhat weaker interaction of this oxygen

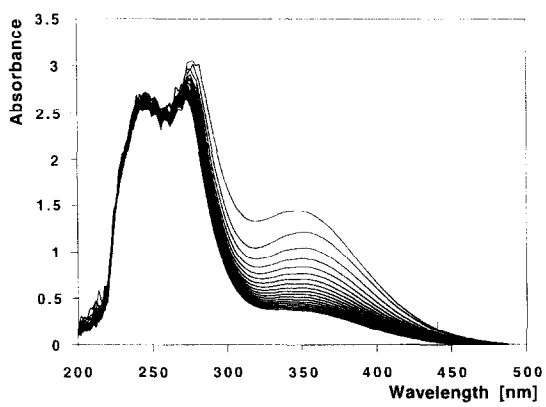

Fig. 5. Time-dependent UV/Vis spectra ($\lambda = 200$–500 nm) of the active species of the system $6/H_2O_2$ (in excess) in THF (decomposition process); $T = 25$°C.

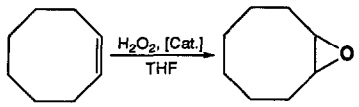

Scheme 6.

donor ligand complex in comparison to *N*-donors. However, the relatively weak interaction O → Re enables the formation of a catalytic active species, which is in remarkable contrast to the behavior of the catalytically inactive systems **7a,b**/H_2O_2 [26,32,33].

Temperature dependence: Examination of the system **6**/H_2O_2 at different temperatures (15–66°C, 0.4 mol% **6**, THF) reveals the activity as a function of the temperature (Fig. 6). Up to ca. 50°C increasing yields and TOF are obtained with higher temperatures. Enhancement of the TOF is still observed above 50°C (TOF(50°C) = 125 1/h), TOF(66°C) = 180 1/h). No increasing yields are obtained above 50°C, which can be explained by a faster decomposition of the catalyst.

Selectivity: The selectivity achieved in the catalytic oxidation of cyclohexene (see above) with the system **6**/H_2O_2 is completely lost at higher temperatures. At 45 and 60°C only 1,2-cyclohexanediol is formed. As in the case of the *cis*-cyclooctene epoxidation the overall yield can be improved using higher temperatures (Fig. 7).

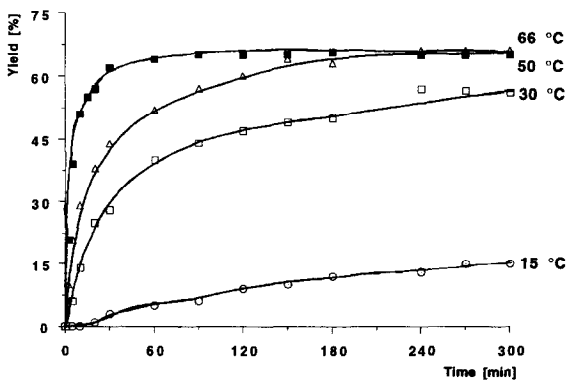

Fig. 6. Catalytic activity of (3-methoxy-*n*-butyl)trioxorhenium (**6**) in the oxidation of *cis*-cyclooctene to epoxycyclooctane with H_2O_2 in THF at different temperatures (15–66°C). *cis*-Cyclooctene: H_2O_2:[Cat.] = 1:1.1:0.004; T = 25°C.

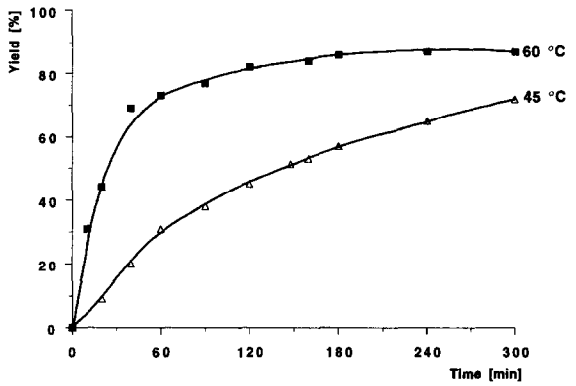

Fig. 7. Catalytic activity of (3-methoxy-*n*-butyl)trioxorhenium (**6**) in the oxidation of cyclohexene to 1,2-hexanediol with H_2O_2 in THF at 45 and 60°C. *cis*-Cyclooctene: H_2O_2:[Cat.] = 1:1.1:0.01.

Addition of *N*-bases such as quinuclidine to the system **6**/H_2O_2 suppresses the oxirane ring-opening but reduces considerably the lifetime of the catalyst. The catalytic activity is completely lost after 30 min, even at room temperature. This result is in good accordance with the catalytic behavior of the long chain alkylrhenium(VII) oxides (e.g., ethyl- and propyltrioxorhenium) [26,29]. The addition of *N*-bases leads to the replacement of the weak O → Re bond by a stronger intermolecular interaction under formation of a base adduct [32]. In this case the intramolecular stabilization of the long alkyl part is no longer valid, the molecule behaves as a base adduct of an alkylrhenium(VII) oxide.

3. Conclusions

N-Oxide complexes of methyltrioxorhenium(VII) (**1**) are easily accessible by reaction of the corresponding *N*-oxide with **1** at low temperatures. Whereas aliphatic *N*-oxide complexes of **1** are instable and not active in catalytic epoxidation of olefins, aromatic *N*-oxide complexes are significantly more stable and highly selective, even in comparison to *N*-base adducts of **1**.

In clear contrast to the intramolecular *N*-donor adducts, the intramolecular *O*-donor adduct **6** is an active and selective epoxidation catalyst. However, above room temperature it looses its selectivity quickly. The selectivity achieved with intermolecular donor adducts of **1** (*N*- and *N*-oxide bases) is higher than that achieved with **6**. The observed catalytic behavior as well as the dimeric solid state structure of **6** is very likely due to the weak donor capability of the oxygen atom in the ether group. A possible way to promote the selectivity of complexes of this type is the addition of strong donor groups to the donating oxygen atom. An improvement of its electron donor capability and consequently a decrease of the Lewis acidity of the rhenium center should thus be observed.

4. Experimental

All reactions were performed using standard Schlenk techniques in an oxygen-free and water-free nitrogen atmosphere. Solvents were dried using standard methods and distilled under N_2. Infrared spectra were recorded as KBr pellets or CH_2Cl_2 solutions on a Perkin–Elmer 1600 series FT-IR instrument (resolution 4 cm^{-1}), the ^1H and ^{17}O NMR spectra at 399.78 and 54.21 MHz, respectively, on a FT-JEOL GX instrument. All NMR solvents were 'freeze-pump-thaw' degassed and stored over molecular sieves prior to use. Elemental analyses were performed at the microanalytical laboratory of our institute. GC/MS data were obtained on a Hewlett Packard 5890 (GC) equipped with a fused-silica column HP-1 (No. 19091Z-102, $l = 50$ m, $\varnothing = 0.2$ mm, thickness of film 0.33 mm) as well as a mass-selective detector HP 5970 B and a FI-detector. The kinetic investigations were performed on a Hewlett Packard 8452A UV/Vis spectrometer coupled to a PC computer (HP 89531A MS-DOS program system), where the data were stored. The measurements were carried out using quartz cuvettes (10 mm light path and 3 ml volume). Solids were weighted on a Sartorius analytical-balance (± 0.0001 g), and liquids were measured with Hamilton syringes. All investigations were performed in cuvettes (various temperatures), and the solutions were diluted to $c < 10^{-2}$ $mol^{-1}\,l^{-1}$. The ^{17}O labelled Lewis-base adducts of methyltrioxorhenium were prepared from **1**–[^{17}O] according to [32,34,35]. Methyltrioxorhenium was prepared according to [40]. For the preparation of **1a** see Refs. [41,42]. **1b** and **1c** were prepared according to [43,44]. Trimethyl *N*-oxide (Aldrich) was used as received. Quinuclidine *N*-oxide, 4-*tert*-butylpyridine *N*-oxide, and rac-[1-(6-bromopyridine-2-yl *N*-oxide)-2,2-dimethylpropyl]methyl ether were prepared from the corresponding amines according to [45]. For the preparation of rac-[1-(6-bromopyridine-2-yl)-2,2-dimethylpropyl]methyl ether see [46]. **6** was prepared as described in [32].

*4.1. Preparation of the N-oxide adducts of methyltrioxorhenium (**3a**, **3b**, **3c**, **3d**)*

*4.1.1. Synthesis of (trimethyl N-oxide)methyltrioxorhenium(VII) (**3a**)*

Trimethyl *N*-oxide (0.1 g, 0.76 mmol) was added to a solution of methyltrioxorhenium(VII) (**1**) (0.19 g, 0.76 mmol) in 10 ml acetonitrile at -10°C. After 10 min a yellow solid precipitated, and the reaction was allowed to react for additional 30 min. The solution was then concentrated at -10°C to ca. 2 ml. After filtration of the mother liquor the yellow residue was washed with cold diethyl ether (3×5 ml) and dried in oil pump vac. at -10°C. Yield: 0.19 g (0.60 mmol, 79%).

Elemental analysis: Calcd. for $C_4H_{12}N_1O_4Re_1$ (324.34): C, 14.81; H, 3.72; N, 4.32. Found: C, 14.85; H, 3.43; N, 4.39.

Spectroscopic data: IR [KBr, cm^{-1}] $\nu = 2922$ (w); 2894 (w); 2851 (w); ν(N–O–Re) 1477 (m); 1065 (m); 1013 (s); ν_{sym}(Re=O) 970 (w); ν_{asym}(Re=O) 935 (vs); 821 (w); 645 (w).

4.1.2. (Quinuclidine N-oxide)methyltrioxorhenium(VII) (3b)

Quinuclidine *N*-oxide · $4H_2O$ (0.15 g, 1.2 mmol) was added to a solution of methyltrioxorhenium(VII) (**1**) (0.3 g, 1.2 mmol) in 5 ml acetonitrile −30°C. After 10 min a pale-yellow solid precipitated. The reaction was allowed to react for additional 10 min, and the solvent was filtered off. The solid was washed with cold diethyl ether (3 × 5 ml) and dried in oil pump vac. at −10°C. Yield: 0.370 g (0.98 mmol, 82%).

Elemental analysis: Calcd. for $C_8H_{16}NO_4Re$ (376.39): C, 25.52; H, 4.25; N, 3.72. Found: C, 25.26; H, 4.33; N 3.72.

Spectroscopic data: IR [KBr, cm^{-1}] ν = 2965 (w); 2888 (w); ν(N–O–Re)1466 (w);1407 (w); 1354 (w); 1057 (w); ν_{sym} (Re=O) 960 (vw); ν_{asym} (Re=O) 916 (vs); 568 (m). ^{1}H–NMR [$CDCl_3$, 399.80 MHz, 25°C, ppm]: δ(N($CH_2CH_2)_3CH$) 1.96 [s, 7H]; δ(Re–CH_3) 2.14 [s, 3H]; δ(N($CH_2CH_2)_3CH$) 3.45 [s, 6H]. ^{13}C–NMR [$CDCl_3$, 100.51 MHz, 25°C, ppm]: δ(N($CH_2CH_2)_3CH$) 19.8; δ(N(CH_2CH_2)CH) 26.1; δ(Re–CH_3) 30.9; δ(N(CH_2CH_2)CH) 60.8. ^{17}O–NMR [$CDCl_3$, 54.2 MHz, 25°C, ppm]: δ(Re=O) 835.

4.1.3. (4-tert-butylpyridine N-oxide)methyltrioxorhenium(VII) (3c)

4-*tert*-Butylpyridine *N*-oxide (0.15 g, 1.0 mmol) was added to a solution of methyltrioxorhenium(VII) (**1**) (0.25 g, 1.0 mmol) in 10 ml diethyl ether at 0°C. After 1 min a pale-yellow solid precipitated. After 10 min the solvent was filtered off and the remaining yellow solid was washed with diethyl ether (3 × 5 ml). The obtained compound was then dried in oil pump vac. Yield: 0.36 g (0.98 mmol, 98%).

Elemental analysis: Calcd. for $C_{10}H_{16}NO_4Re$ (368.45): C, 30.00; H, 4.00; N, 3.50. Found: C, 29.99; H, 4.14; N, 3.47.

Spectroscopic data: IR [KBr, cm^{-1}] ν = 3118 (w); 3087 (w); 2969 (m); ν(N–O–Re) 1489 (s); 1223 (m); 1208 (m); 1178 (m); ν_{sym} (Re=O) 968 (w); ν_{asym} (Re=O) 928 (vs); 848 (m); 821 (m); 681 (w); 558 (w). ^{1}H–NMR [CD_3CN, 399.80 MHz, 25°C, ppm]: δ(C($CH_3)_3$) 1.33 [s, 9H]; δ(Re–CH_3) 1.90 [s, 3H]; δ(N–CH–C*H*) 7.62–7.63 [m, 2H]; δ(N–C*H*–CH) 8.13–8.15 [m, 2H]. ^{13}C–NMR [CD_3CN, 100.51 MHz, 25°C, ppm]: δ(Re–CH_3) 24.38; δ(C($CH_3)_3$) 30.40; δ(($C(CH_3)_3$) 35.98; δ(N–CH–*C*H) 125.00; δ(N–CH–CH–*C*) 140.80; δ(N–CH) 159.84. ^{17}O–NMR [$CDCl_3$, 54.2 MHz, 25°C, ppm]: δ(Re=O) 838.

4.1.4. [Rac-{1-(6-bromopyridine-2-yl N-oxide)-2,2-dimethylpropyl}methyl ether]methyltrioxorhenium(VII)(3d)

Rac-[1-(6-bromopyridine-2-yl *N*-oxide)-2,2-dimethylpropyl]methyl ether (0.163 g, 0.66 mmol) dissolved in 3 ml of CH_2Cl_2 was added dropwise to a solution of methyltrioxorhenium(VII) (0.150 mg, 0.60 mmol) in 3 ml diethyl ether at −35°C. After ca. 15 min a white solid precipitated. The reaction was allowed to react for additional 30 min. The white solid, obtained after filtration, was washed with diethyl ether (3 × 5 ml), and dried in oil pump vac. Yield: 0.236 g (0.45 mmol, 75%).

Elemental analysis: Calcd. for $C_{12}H_{19}BrNO_5Re$ (523.44): C, 27.54; H, 3.66; N, 2.67; Br 15.26. Found: C, 27.72; H, 3.68; N, 2.71; Br, 15.46.

Spectroscopic data: IR ν [KBr, cm^{-1}] = 3546 (m); 3477 (m); 3414 (m); 2969 (s); 2939 (s); 1602 (w); 1558 (w); ν(N–O–Re) 1460 (s); 1395 (s); 1343 (s); 1326 (s); 1195 (s); 1173 (s); 1092 (vs); ν_{sym}(Re=O) 967 (s); ν_{asym}(Re=O) 930 (vs); 829 (s); 806 (s); 785 (s); 708 (s); 588 (s): ^{1}H–NMR [$CDCl_3$, 399.80 MHz, 25°C, ppm]: δ(C($CH_3)_3$) 0.94 [s, 9H]; δ(Re–CH_3) 2.54 [s, 3H]; δ(OCH_3) 3.20 [s, 3H]; δ(C*H*) 4.99 [s, 1H], δ(H4) 7.10 [t, 1H, ^3J(H,H) = 7.93 Hz]; δ(H3) 7.37 [dd, 1H, ^3J(H,H) = 7.94 Hz, ^4J(H,H) = 1.22]; δ(H5) 7.58 [dd, 1H, ^3J(H,H) = 7.94 Hz, ^4J(H,H) = 1.22 Hz]. ^{13}C–NMR [$CDCl_3$, 100.51 MHz, 25°C, ppm]: δ(Re–CH_3) 19.5; δ(C($CH_3)_3$) 25.6; δ($C(CH_3)_3$) 37.3;

δ(*C*H)58.1; δ(OCH_3) 83.4, δ(C3) 124.2; δ(C4) 124.7; δ(C5) 128.9; δ(C2) 133.8; δ(C6) 53.6.

4.2. General procedure for the catalytic epoxidation with complexes 3a–3d

The catalyst (0.12 mmol) and cyclooctane (1.00 g, internal standard) were dissolved in a 10% H_2O_2 solution in *t*BuOH (6.2 ml, 18.3 mmol, prepared according to [26]). In the case ligands were used, they were added (0.72 mmol) to the solution prior to substrate addition. The temperature was brought to 25 ± 1°C and kept at this value for the specified times. Cyclohexene (1.016 g, 12.17 mmol) was then added. The reaction was monitored by GC.

4.3. General procedure for the catalytic epoxidation with complex 6

0.5–1 mol% of **6** were dissolved in 10 ml THF and brought to the desired temperature (± 1°C). Di-*n*-butyl ether (cyclooctene oxidation) and cycloctane (cycloctene oxidation) were added as internal standards. 3.5 ml (10 mmol) of a 10% H_2O_2 solution in THF was added and the solution turned yellow within a couple of minutes. 9 mmol of the corresponding substrate was then added. The reaction was monitored by GC.

4.4. X-ray structure determinations of 3c and 6

Both crystals were prepared under air in a Lindemann glass capillary. All data were collected with graphite monochromatized Mo-K_α radiation on an Enraf-Nonius CAD4 diffractometer. Final cell constants were obtained by least-squares refinement of 25 automatically centered reflections (**3c**: $30.1° < 2\Theta < 36.0°$, **6**: $27.2° < 2\Theta < 36.1°$). Data were collected in the ω-scan mode. Orientation control reflections were monitored every 100 reflections, intensity control reflections were monitored every 60 minutes. All data sets were corrected for Lorentz and polarization terms. A decay in intensity of 4.4% was corrected for **3c**. An empirical absorption correction (ψ-scans) was applied to both data sets. No extinction correction was necessary. Crystal data and refinement parameters are summarized in Table 1.

Table 1
Crystallographic data of **3c** and **6**

	3c	**6**
Formula	$C_{10}H_{16}N_1O_4Re_1$	$C_{10}H_{22}O_8Re_2$
f_w (g mol^{-1})	400.44	642.69
Crystal	yellow fragment	yellow fragment
Crystal size (mm^3)	0.18·0.26·0.38	0.10·0.15·0.20
Space group	P 2_1/n (No. 14)	P 2_1/n (No. 14)
a (pm)	757.1(2)	740.7(3)
b (pm)	910.00(7)	706.8(1)
c (pm)	1916.2(4)	1492.2(5)
β (°)	99.909(9)	97.69(2)
V (pm^3)	$1300.5 \cdot 10^6$	$774.1 \cdot 10^6$
D_{calc} (g cm^{-3})	2.05	2.76
Z	4	2
μ (cm^{-1})	94.7	156.5
Temp. (°C)	−50(3)	−50(3)
Measured data	2612	1615
Unique data	2073	1285
Data used	1972	1232
$I/\sigma(I)>$	1.0	1.0
Parameters	145	91
R [a]	0.034	0.028
R_w [b]	0.036	0.029

[a] $R = \Sigma(||F_o| - |F_c||)/\Sigma|F_o|$.
[b] $R_w = [\Sigma w(|F_o| - |F_c|)^2 / \Sigma w F_o^2]^{1/2}$.

The structures were solved by Patterson methods and subsequent difference Fourier techniques [47]. Full-matrix least-squares refinements were carried out by minimizing $\Sigma w(|F_o| - |F_c|)^2$. Hydrogen atoms were calculated in their ideal positions (d_{C-H}: 96 pm, $U_H = 1.3 \cdot U_C$) and included in the data set but not refined. A Chebyshev polynomial weighting scheme was used in all refinements [48]. The refinements were stopped at shift/err < 0.001. The final difference Fourier maps were featureless. All calculations were performed on a MicroVAX 3100 and DECStation 5000/25 computers using the programs or program systems CRYSTALS, STRUX-V, RC93, PLATON, SDP [47–52].

Further details of the crystal structure investigations are available on request from the Fachinformationszentrum Karlsruhe, D-76344 Eggenstein-Leopoldshafen (Germany), on quoting the depository numbers CSD-H405978 (**3c**) and CSD-H405976 (**6**).

4.5. Preparation of methyl(oxo)bis(η^2-peroxo)rhenium(VII) (2c)

4-*tert*-Butylpyridine *N*-oxide (0.227 g, 1.68 mmol) dissolved in 1 ml of CH_2Cl_2 was added dropwise to a solution of **2a** (0.459 g, 1.53 mmol, prepared according to [25]) in 5 ml dry diethyl ether at 0°C. A yellow-orange crystalline product formed immediately. The remaining solvent was filtered off, and the product washed with diethyl ether (2 ×) and pentane (2 ×). The solid was dried in oil pump vac. at 0°C. Yield: 0.509 g (1.17 mmol, 76%). Single crystals were obtained dissolving the compound in a mixture of CH_2Cl_2/diethyl ether (7/2), and cooling down to −30°C.

Elemental analysis: Calcd. for $C_{10}H_{16}NO_6Re$ (432.45): C, 27.71; H, 3.73; N, 3.24; O, 22.18; Re, 43.06; Found: C: 27.82; H; 3.76; N, 3.25; O, 22.03; Re, 42.65.

Melting point: 95–96°C (under decomposition).

Spectroscopic data: IR ν [CH_2Cl_2, cm^{-1}] = ν(N–O–Re) 1492 (s); 1371 (w); 1220 (s); 1182 (m); 1114 (w); ν(Re=O) 992 (vs); $\nu(O_2)$ 871 (m); $\nu(O_2)$ 849 (m); $\nu(O_2)$ 823 (m). ^{1}H–NMR [$CDCl_3$, 399.80 MHz, 25°C, ppm]: δ(C(CH_3)$_3$) 1.32 [s, 9H]; δ(Re–CH_3) 2.89 [s, 3H]; δ(H3,5) 7.37 [d, 2H]; δ(H2,6) 7.82 [d, 2H]. ^{13}C–NMR [$CDCl_3$, 100.51 MHz, 25°C, ppm]: δ(Re–CH_3) 30.28; δ(C(CH_3)$_3$) 31.74; δ(C(CH_3)$_3$) 35.37; δ(C3,5) 122.70; δ(C4) 139.99; δ(C2,6) 160.00. ^{17}O–NMR [$CDCl_3$, 54.2 MHz, 25°C, ppm]: δ(Re=O) 758 (generated in situ).

Acknowledgements

We thank the Deutscher Akademischer Austauschdienst (grant to J.D.G.C.), the Volkswagen foundation, the Deutsche Forschungsgemeinschaft and the Degussa AG for financial and material support. M. Barth of our institute is acknowledged for performing elemental analyses.

References

[1] W.A. Herrmann, D.W. Marz, W. Wagner, J.G. Kuchler, G. Weichselbaumer and R.W. Fischer, DE 3.902.357, Jan. 27, 1989; EP 90101439.9, Jan. 25, 1990.
[2] W.A. Herrmann, R.W. Fischer and D.W. Marz, Angew. Chem. 103 (1991) 1706 Angew. Chem. Int. Ed. Engl. 30 (1991) 1638.
[3] W. Adam, W. Haas and B.B. Lohray, J. Am. Chem. Soc. 113 (1991) 6202.
[4] W. Adam and B.B Lohray, J. Am. Chem. Soc. (1996) (in press).
[5] S. Yamazaki, J.H. Espenson and P. Houston, Inorg. Chem. 32 (1993) 4685.
[6] P. Houston, J.H. Espenson and A. Bakac, Inorg. Chem. 32 (1993) 4517.
[7] V.A. Vassell and J.H. Espenson, Inorg. Chem. 33 (1994) 5491.
[8] J.H. Espenson, P. Houston, O. Petrousky and S. Staudt, J. Am. Chem. Soc. 116 (1994) 2689.
[9] M.M. Abu-Omar and J.H. Espenson, 34 (1995) 6239.
[10] P.J. Hansen and J.H. Espenson, Inorg. Chem. 34 (1995) 5839.
[11] A.M. Al-Ajlouni and J.H. Espenson, J. Am. Chem. Soc. 117 (1995) 9243.
[12] Z. Zhu and J.H. Espenson, J. Org. Chem. 60 (1995) 1326.
[13] K.A. Vassell and J.H. Espenson, Inorg. Chem. 33 (1994) 5491.
[14] E.I. Karasevich, A.V. Nikitin and V.L. Rubailo, Kinet. Catal. 35 (1994) 810.
[15] S. Yamazaki, Chem. Lett. (1995) 127.
[16] W.A. Herrmann, P.W. Roesky, W. Scherer and M. Kleine, Organometallics 13 (1994) 4536.
[17] W.A. Herrmann, R.W. Fischer and J.D.G. Correia, J. Mol. Catal. 94 (1994) 213.
[18] W.A. Herrmann, J.D.G. Correia, R.W. Fischer, W. Adam, J. Lin and Ch.R. Saha-Möller, DE P44197993, 1994 (HOECHST AG).
[19] W.A. Herrmann, W. Adam, J. Lin, Ch.R. Saha-Möller, R.W. Fischer and J.D.G. Correia, Angew. Chem. 106 (1994) 2545; Angew. Chem. Int. Ed. Engl. 33 (1994) 2475.
[20] A. Thome, M. Roeper and H.-J. Kneuper, DE 4228887 v. 29.8. 1992 (BASF AG).
[21] W.A. Herrmann, W. Wagner, U. Flessner, U. Volkhardt and W. Komber, Angew. Chem. 103 (1991) 1704; Angew. Chem. Int. Ed. Engl. 30 (1991) 1636.
[22] W.A. Herrmann, W. Wagner and U. Volkhardt, DE 3940196, Dec. 5, 1988, and EP 891224370, Nov. 5, 1988 (HOECHST AG).
[23] W.A. Herrmann and M. Wang, Angew. Chem. 103 (1991) 1709; Angew. Chem. Int. Ed. Engl. 30 (1991) 1641.

[24] W.A. Herrmann, P.W. Roesky, M. Wang and W. Scherer, Organometallics 13 (1994) 4531.
[25] W.A. Herrmann, R.W. Fischer, W. Scherer and M.U. Rauch, Angew. Chem., 105 (1993) 1209; Angew. Chem. Int. Ed. Engl. 32 (1993) 1157.
[26] W.A. Herrmann, R.W. Fischer, M.U. Rauch and W. Scherer, J. Mol. Catal. 86 (1994) 243.
[27] W.A. Herrmann, recent review, J. Organomet. Chem., 500 (1995) 149.
[28] W.A. Herrmann, J.D.G. Correia, G.R.J. Artus, R.W. Fischer and C.C. Romão, J. Organomet. Chem. 520 (1996) 139.
[29] W.A. Herrmann, F.E. Kühn, C.C. Romão, H. Tran Huy, M. Wang, R.W. Fischer, W. Scherer and P. Kiprof, Chem. Ber. 26 (1993) 45.
[30] W.A. Herrmann, C.C. Romão, R.W. Fischer, P. Kiprof and C. de Méric de Bellefon, Angew. Chem. 103 (1991) 183; Angew. Chem. Int. Ed. Engl. 30 (1991) 185.
[31] W.A. Herrmann, J.D.G. Correia, F.E. Kühn and G.R.J. Artus, Chem. Eur. J. 2 (1996) 168.
[32] W.A. Herrmann, F.E. Kühn, M.U. Rauch, J.D.G. Correia and G. Artus, Inorg. Chem. 34 (1995) 2914.
[33] M.U. Rauch, Ph.D. Thesis (Munich, 1996).
[34] W.A. Herrmann, F.E. Kühn and P.W. Roesky, J. Organomet. Chem. 485 (1995) 243.
[35] F.E. Kühn, Ph.D. Thesis (Munich, 1994).
[36] W.A. Herrmann, P.W. Roesky, M. Wang and W. Scherer, Organometallics 13 (1994) 4536.
[37] C. de Méric de Bellefon, W.A. Herrmann, P. Kiprof and C.R. Whitaker, Organomerallics 11 (1992) 1072.
[38] J. Mink, G. Keresztury, A. Stirling and W.A. Herrmann, Spectrochim. Acta 50A (1994) 2039.
[39] W.A. Herrmann, B.A. Woijtczak, F.E. Kühn, G.R.J. Artus and M.M. Mattner, Inorg. Chem. (1996), in press.
[40] W.A. Herrmann, F.E. Kühn, R.W. Fischer, W.R. Thiel and C.C. Romão, Inorg. Chem. 31 (1992) 4431.
[41] W.A. Herrmann, J.G. Kuchler, G. Weichselbaumer, E. Herdtweck and P. Kiprof, J. Organomet. Chem. 372 (1989) 351.
[42] W.A. Herrmann, G. Weichselbaumer and E. Herdtweck, J. Organomet. Chem. 372 (1989), 371.
[43] W.A. Herrmann, P.W. Roesky, R. Alberto, G.R.J. Artus and W. Scherer, Inorg. Chem. (submitted).
[44] P.W. Roesky, Ph.D. Thesis (Munich, 1994).
[45] J.D.G. Correia, Ph.D. Thesis (Munich, 1996).
[46] C. Bolm, M. Ewald, M. Felder and G. Schlingloff, Chem. Ber. 125 (1992) 1169.
[47] D.J. Watkin, P.W. Betteridge and J.R. Carruthers, Crystals (Oxford Univ. Computing Lab., 1986).
[48] J.R. Carruthers and D.J. Watkin, Acta Crystallogr. A 35 (1979) 698.
[49] G.R.J. Artus, W. Scherer, T. Priermeier and E. Herdtweck, STRUX-V (Technische Univ. München, 1994).
[50] P. Lilley, RC93 (Oxford Univ. Computing Lab., 1993/1994).
[51] A.L. Spek, PLATON-93, Acta Crystallogr. A 46 (1990) C34.
[52] B.A. Frenz, ENRAF-NONIUS "SDP" Version 4.0 (Delft, 1988).